

Frequency of Sahelian storm initiation enhanced over mesoscale soil-moisture patterns

Christopher M. Taylor^{1*}, Amanda Gounou², Françoise Guichard², Phil P. Harris¹, Richard J. Ellis¹, Fleur Couvreur² and Martin De Kauwe³

1 Evapotranspiration of soil moisture can affect temperature and humidity in the lower atmosphere, and thereby the development of convective rain storms. Climate models have illustrated the importance of soil moisture-precipitation feedbacks for weekly rainfall totals in semi-arid regions, such as the Sahel¹. However, large variations exist between model feedbacks, and the mechanisms governing the strength and sign of the feedback are uncertain. Here, we use satellite observations of land surface temperatures and convective cloud cover over West Africa—collected during the wet seasons between 2006 and 2010—to determine the impact of soil moisture on rainfall in the Sahel. We show that variations in soil moisture on length scales of approximately 10–40 km exert a strong control on storm initiation—as evidenced by the appearance of convective cloud. The probability of convective initiation is doubled over strong soil moisture gradients compared to that over uniform soil moisture conditions. We find that 37% of all storm initiations analysed occurred over the steepest 25% of soil moisture gradients. We conclude that heterogeneities in soil moisture on scales of tens of kilometres have a pronounced impact on rainfall in the Sahel, and suggest that similar processes may be important throughout the semi-arid tropics.

This study focuses on the impact of soil moisture on rainfall in the Sahel, a semi-arid region bounded to the north by the Sahara desert and to the south by closed canopy tropical forest. The region receives almost all its annual rain in the summer wet season associated with the northward excursion of the Inter-Tropical Convergence Zone under the influence of the West African Monsoon². A strong seasonal cycle in vegetation peaks in September, about three weeks after the climatological peak in rainfall. The region experiences extreme droughts by global standards, with profound consequences for the local population. Modelling studies have illustrated how rainfall anomalies induced by oceanic variability are amplified by a feedback with Sahelian soil moisture and vegetation^{3–5}. Climate models suggest soil moisture feedbacks on time scales of days are relatively strong in the Sahel¹, a fact supported by observational evidence^{6,7}. However, it is unclear which atmospheric processes control the strength, and even the sign of the feedbacks operating at different spatial scales.

Feedbacks are relatively easy to observe in the Sahel. There is strong natural variability in soil moisture on a daily timescale, driven by convective rain events, and followed by drying of the top centimetres of the soil. This soil moisture variability induces strong variations in surface fluxes in the days after rain because of the sparseness of the vegetation⁸. Accurate estimates of rainfall and

surface fluxes do not exist on the scales at which land-convection feedbacks operate, but satellite data can provide valuable proxies. The presence of cold cloud, in particular when organized into extensive Mesoscale Convective Systems (MCS), provides a means to examine relationships between convection and the land surface from a statistical perspective. These long-lived travelling systems produce 80–90% of the annual rain in the region⁹, and the seasonal total of MCS account for the difference between a wet and a dry year¹⁰. For characterizing surface flux variability we use two independent proxies. Surface soil moisture estimates¹¹ are available, typically daily, from a passive microwave sensor with a footprint ~ 40 km. For finer spatial resolution, we exploit land surface temperature (LST) data, available by geostationary satellite every 15 min under clear sky at a resolution of 3 km (ref. 12). Sahelian soil wetting and drying cycles create strong anomalies in LST (henceforth LSTA) on a daily timescale. We use variability in daytime mean LSTA as a proxy for surface fluxes with negative anomalies indicative of increased evaporation and reduced sensible heat flux. Some characteristics of spatial variability in LSTA are provided in the Supplementary Fig. S5. Aircraft measurements made during the African Monsoon Multidisciplinary Analysis (AMMA) campaign^{13–15} have demonstrated that gradients in LSTA coincide with horizontal gradients in the Planetary Boundary Layer at wavelengths as low as 5–10 km (ref. 13). They provided conclusive observational evidence that antecedent rain can generate mesoscale convergence zones, even at wavelengths of 20 km, consistent with modelling studies^{16–21}. These convergence zones are important for their potential impact on the development of moist convection, a feedback process observed for a single case during AMMA (ref. 14).

We examined the impact of the land surface on the initiation of MCS using a dataset of 3,765 storms, within a region ~ 2.5 million km² (10° W–10° E, 10°–20° N) for the 2006–2010 wet seasons. We tracked convective cloud areas using commonly-adopted thresholds of brightness temperature and areal extent (see Methods). We defined an MCS initiation event when a cold cloud first appeared, before expansion into an MCS. This definition allowed us to assess where deep convection was triggered relative to the underlying surface. Our study covers the afternoon–evening period (1200–2100 UTC) when over 80% of MCS are initiated²².

Figure 1 shows the number of MCS initiations identified as a function of land surface properties, on a regular grid of $0.35 \times 0.35^\circ$ (approximately 40×40 km²). The probability of initiation (P_i) for different soil moisture conditions at this scale (Fig. 1a) provides no clear evidence for a link between soil moisture and MCS initiation. However, a strong relationship emerges when one considers mesoscale anomalies in soil moisture (Fig. 1b). Within

¹Centre for Ecology and Hydrology, Wallingford, UK, ²CNRM (CNRS and Météo-France), Toulouse, France, ³Macquarie University, Sydney, Australia.
*e-mail: cmt@ceh.ac.uk

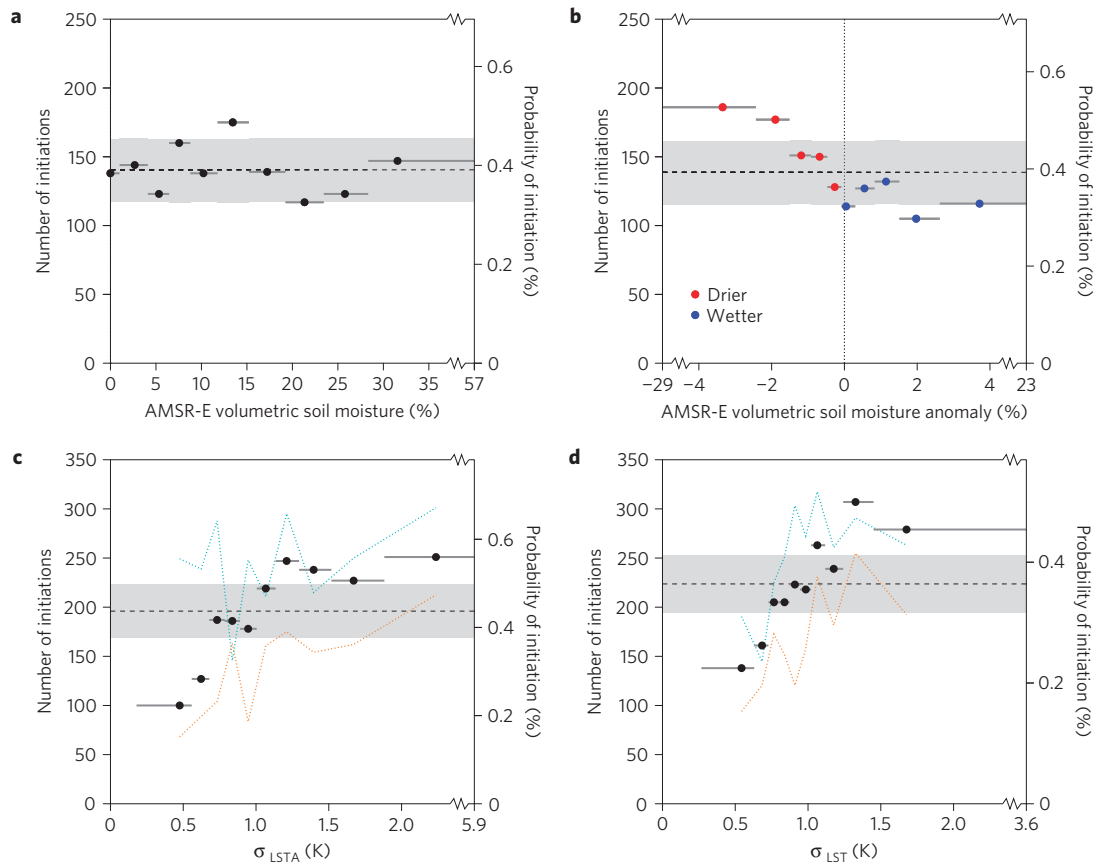


Figure 1 | Sensitivity of MCS initiation to land surface properties. Total number and probability of initiations as a function of (a) volumetric soil moisture (b) volumetric soil moisture anomaly compared to the mean over $1.75^\circ \times 1.75^\circ$, (c) σ_{LSTA} , and (d) σ_{LST} . Each horizontal line represents one decile, a circle indicates the median, and shading delimits the 95% confidence limits. In c and d, the probability of initiation is also shown for sub-samples containing grid points with $dp_{LFC} < 210$ hPa (blue line) and $dp_{LFC} > 300$ hPa (orange line). The relationships in c and d are independent, as σ_{LSTA} is not correlated with σ_{LST} ($r = 0.018, n > 50,000$).

1 an area of approximately 200×200 km², the size of a typical
 2 climate model grid box, the probability of storm initiation is
 3 about one third higher over drier soils compared to wet areas.
 4 This relationship is consistent with previous studies looking at
 5 both Sahelian soil moisture⁶, and land cover in other regions^{23,24},
 6 where afternoon convection is favoured over surfaces with a greater
 7 sensible heat flux.

8 To assess the relevance of finer-scale soil moisture patterns
 9 in the initiation process, we examined the spatial variability of
 10 LSTA within each 40 km grid box by computing the standard
 11 deviation (σ_{LSTA}) of the 3 km pixels within. The value of P_1 increases
 12 strongly with soil moisture heterogeneity (Fig. 1c; $\chi^2 = 119, df =$
 13 $9, P < 0.0001$). Comparing the number of initiations in the lowest
 14 decile with the highest decile, P_1 increases by a factor of 2.5. This
 15 relationship is robust to the methods used to compute the LSTA,
 16 but is sensitive to the choice of grid box size (Supplementary Fig.
 17 S1). In particular, the rise in P_1 with σ_{LSTA} is maximized for grid
 18 boxes of lengths less than 30 km, and becomes weak for grid boxes
 19 of 100 km or larger. The sensitivity of P_1 to σ_{LSTA} under different
 20 thermodynamic conditions was also assessed (Fig. 1c) using the
 21 pressure difference between the level of free convection (LFC) and
 22 the surface (dp_{LFC}) computed from atmospheric analyses. When
 23 the atmosphere is conducive to deep convection ($dp_{LFC} < 210$ hPa),
 24 values of P_1 are high, yet there is no clear increase with σ_{LSTA}
 25 ($\chi^2 = 8.32, df = 9, P = 0.50$). On the other hand, when convective
 26 inhibition is large ($dp_{LFC} > 300$ hPa), the sensitivity to σ_{LSTA}
 27 is stronger, with a threefold increase in P_1 between the lowest
 28 and highest deciles. This strong sensitivity under unfavourable

large-scale atmospheric conditions implies that mesoscale soil
 moisture patterns trigger MCS which would not otherwise occur.

Mesoscale flux variability can originate from fixed landscape
 features as well as transient soil moisture patterns. The impact of
 these fixed features on MCS initiation was quantified using the
 standard deviation in the wet season mean LST (σ_{LST} ; Fig. 1d).
 Grid boxes with sub-grid variations in topographic height exceeding
 250 m were excluded from this calculation to avoid the well-known
 orographic effect on initiation. Whilst large values of σ_{LST} are less
 common than for σ_{LSTA} in the study region, the relationships with
 P_1 are consistent for both fixed and transient heterogeneity (Fig. 1c
 and d). The highest values of σ_{LST} were found over crop/forest areas
 in the south²⁵, and rocky areas associated with the Continental
 Terminal in the north.

The mean mesoscale structure of the LSTA field was determined
 by compositing the 3,765 initiations relative to the low-level
 wind direction provided by atmospheric analyses (Fig. 2a). This
 indicates favoured initiations within an elliptical pattern of positive
 LSTA values aligned with the background wind. Notable negative
 gradients in the composite-mean LSTA are evident about 10 km
 from the initiation point in the down-wind and both cross-wind
 directions, corresponding to transitions to wetter soil. The
 composite soil moisture field from passive microwave is consistent
 with the LSTA field, although rather poorly resolved by comparison.
 To assess the preferred surface length scales, we performed a wavelet
 analysis on along-wind LSTA transects for every initiation. The
 average of these wavelets reveals strong variability on wavelengths
 of 20–75 km centred 0–10 km downwind of initiation (Fig. 2b).

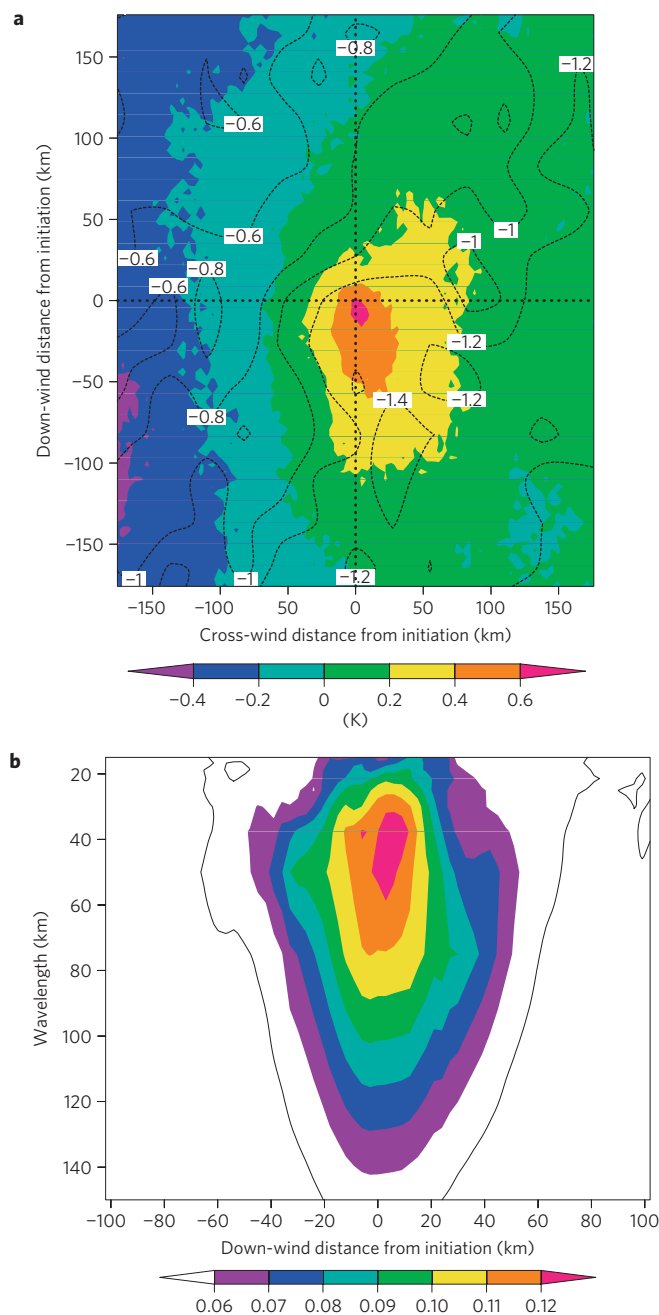


Figure 2 | Mesoscale surface variability around initiation point.

a, Composite LSTA (K; shading) and volumetric soil moisture anomalies from the seasonal mean (%; contours). For clarity, the spatial mean LSTA was removed from each event. Anomalies larger than ± 0.2 K are statistically different from 0 (2-tailed *t* test, $P < 0.01$ for $n = 2,439$).

b, Weighted wavelet Z-transform²⁸ computed from LSTA transects in the along-wind direction. The shading denotes the difference in the mean between the initiation and a control (non-initiation) dataset. Within the black contour line, the increase in amplitude between the two datasets is significant ($P < 0.01$) according to a 1-tailed *t*-test.

1 We further examined the likelihood of finding strong LSTA
 2 gradients 10 km downwind of initiation in each case and compared
 3 this with the distribution of LSTA gradients found by random
 4 sampling in the region (see Methods). The distribution in the
 5 initiation sample is shifted to the left relative to the control (Fig. 3).
 6 We calculated the LSTA gradient intervals corresponding to the
 7 first and central deciles (0–10% and 45–55%, respectively) of the

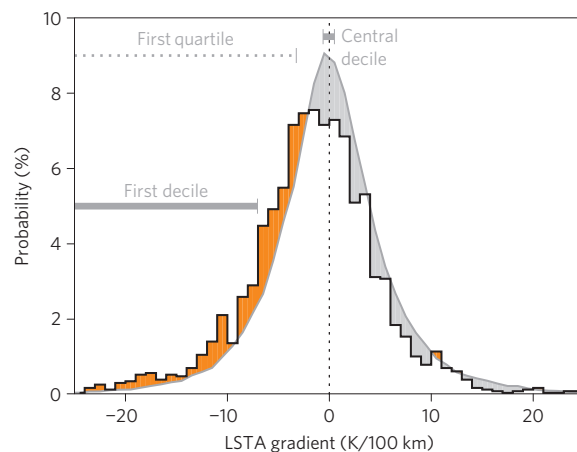


Figure 3 | Distribution of LSTA gradients associated with MCS initiations.

The frequency of along-wind LSTA gradients (K/100 km) located 10 km downstream of the initiation point (black stepped line). The expected frequency of gradients found by sampling across the region (see Methods) is shown for comparison (grey line) with areas of enhanced (reduced) probability of initiation shaded in orange (grey).

control sample, which by definition are observed equally frequently. Convective initiations within the lowest interval occur 2.0 times more frequently than in the central interval. Thus, initiations are twice as likely over strong LSTA gradients compared to uniform surface conditions (the lowest and central intervals respectively). Furthermore, we found that 37% of all the initiations occurred over moderately strong negative gradients (< -3.2 K/100 km), corresponding to the first quartile of the control sample. This enhancement of initiations is equivalent to one in 8.3 of all MCS in the dataset.

The feedback is evident throughout the wet season, with differences in the distributions significant at $P < 0.0001$ for the four individual months as well as for the wet season mean (Supplementary Fig. S4). However, the effect is most pronounced in June and weakest in August. Two factors are likely to determine this seasonality. During the core monsoon period (July/August), the LFC tends to be lower, a regime where convective sensitivity to the surface is weaker (Fig. 1). Second, spatial contrasts in fluxes tend to weaken as the season progresses, because the developing vegetation can maintain transpiration rates over dry spells⁸.

Modelling studies have shown²⁶ that convection is favoured over dry soils, but close to negative upwind gradients in sensible heat flux. This preferred configuration occurs because convergence is maximized where the large-scale wind opposes the shallow surface-induced flow, as summarized in Fig. 4. Strong evidence that such soil moisture-induced circulations do favour storm initiation is provided by our results, in particular, the composite surface structure depicted in Fig. 2a. The preferred initiation point in our observations is consistent with model studies, that is, just upwind of a dry–wet surface transition.

This study shows that soil moisture heterogeneity on scales of tens of kilometres has a pronounced impact on rainfall at the larger scale in the Sahel. This upscaling occurs because, once the convective instability has been released, the MCS expands and propagates typically hundreds of kilometres. The new soil wetness patterns produced by an MCS in turn increase the probability of another MCS in the following day or two. We estimate spatial variability in LSTA on the day following a storm to be increased from 1.0 to 1.6 K (Supplementary Fig. S3), leading to positive feedback on the MCS scale of hundreds of kilometres. On the other hand, considering smaller scales of several tens of kilometres, the feedback is negative owing to preferred triggering over dry soils.

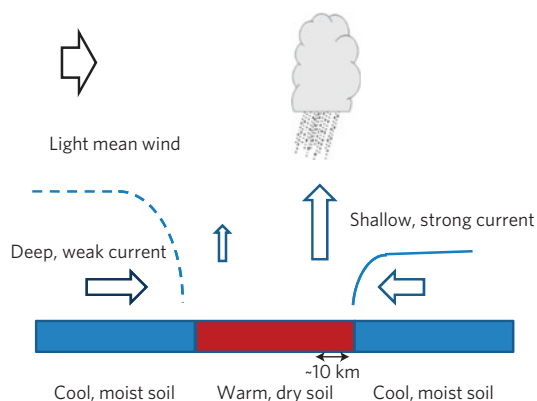


Figure 4 | Schematic depicting the impact of soil moisture heterogeneity on convective initiation. Idealized soil moisture-induced flows (blue arrows) under light synoptic winds create an ascent region where the shallow, strong current opposes the mean wind (adapted from Fig. 7 in ref. 25). The preferred location for convective initiation in this study coincides with the ascent region induced by the heating gradient at the downwind edge of the dry patch. Additional convergence over the dry patch is provided by a deep, weaker current at its upwind edge, and cross-wind gradients in soil moisture (evident in Fig. 2a but not shown here).

The observed relationships between convective initiation and soil moisture patterns presented here shed new light on land–atmosphere coupling mechanisms in the real world. Though focused on the Sahel, the conclusions are likely to be relevant for many semi-arid regions, particularly in the tropics, where a short growing season is driven by the seasonal migration of the ITCZ. It is important to note that the feedbacks highlighted here occur on length scales which are not represented in current climate models, although their effects have large scale consequences. This raises questions about the sensitivity of climate models to soil moisture, and their predictions for future rainfall changes in the semi-arid tropics.

Methods

We used thermal infra-red brightness temperature data from the 10.8 μm channel on the Meteosat Second Generation series of satellites, available every 15 min at a spatial resolution ~ 3 km. We adopted the widely used threshold of -40°C to denote cold cloud. An MCS was defined as an area of contiguous cold cloud exceeding 5,000 km^2 . When an MCS was found which did not overlap with an MCS in the previous time step, we tracked the cold cloud system back in time and space to its origins. Provided the first cold pixel occurred a maximum of 3 h before the areal MCS threshold being crossed, and that it did not overlap with other MCS during that time, we defined the location of that first cold pixel to be the initiation point of the MCS. The results of our simple MCS detection algorithm were very similar to those produced by a more complex tracking method²⁷.

To calculate values of LSTA, we applied a cloud screening to the LST data¹³. We then computed a mean diurnal cycle based on all remaining data within a period of 21 days, centred on the day in question. Daily LSTA were determined by averaging the diurnal LST anomalies between 8 and 16 UTC.

We used operational analyses from the European Centre for Medium Range Weather Forecasting for an estimate of synoptic conditions in the vicinity of MCS initiations. These data have a horizontal resolution of 0.35° and comprise 50 vertical levels between the surface and 15 km. The low level wind data was taken at 10 m above the ground from the 12 UTC analyses, whilst the LFC was estimated at 06 UTC by lifting a parcel from about 50 m above the ground.

The confidence limits in Fig. 1 were calculated based on a binomial distribution, where the probability of initiation was determined from the observations before binning. A χ^2 test was performed on the histograms in Fig. 1c under the null hypothesis that they were uniform. In Fig. 3, we sampled the background distribution of LSTA gradients on the day in question using 44 regularly spaced locations around each initiation point. These points occurred every 0.5° within a $4^\circ \times 2^\circ$ lattice. This sampling strategy ensured that the gradients were appropriately weighted by latitude and day of year. Only soil moisture data from descending orbits of the Aqua satellite were used (overpass time around 0130 UTC), and data excluded where rain exceeding 2 mm was detected in the TRMM3B42 dataset for the hours between the overpass and midday.

Received 3 December 2010; accepted 4 May 2011; published online XX Month XXXX

References

- Koster, R. D. *et al.* Regions of strong coupling between soil moisture and precipitation. *Science* **305**, 1138–1140 (2004).
- Hastenrath, S. *Climate Dynamics of the Tropics* (Kluwer, 1995).
- Ganopolski, A. *et al.* The influence of vegetation–atmosphere–ocean interaction on climate during the mid-Holocene. *Science* **280**, 1916–1919 (1998).
- Zeng, N., Neelin, J. D., Lau, K. M. & Tucker, C. J. Enhancement of interdecadal climate variability in the Sahel by vegetation interaction. *Science* **286**, 1537–1540 (1999).
- Giannini, A., Saravanan, R. & Chang, P. Oceanic forcing of Sahel rainfall on interannual to interdecadal time scales. *Science* **302**, 1027–1030 (2003).
- Taylor, C. M. & Ellis, R. J. Satellite detection of soil moisture impacts on convection at the mesoscale. *Geophys. Res. Lett.* **33**, L03404 (2006).
- Taylor, C. M. & Lebel, T. Observational evidence of persistent convective-scale rainfall patterns. *Mon. Weather Rev.* **126**, 1597–1607 (1998).
- Kohler, M., Kalthoff, N. & Kottmeier, C. The impact of soil moisture modifications on CBL characteristics in West Africa: A case-study from the AMMA campaign. *Q. J. R. Meteorol. Soc.* **136**, 442–455 (2010).
- Mathon, V., Laurent, H. & Lebel, T. Mesoscale convective system rainfall in the Sahel. *J. Appl. Meteorol.* **41**, 1081–1092 (2002).
- Lebel, T., Taupin, J. D. & D'Amato, N. Rainfall monitoring during HAPEX-Sahel: 1. General rainfall conditions and climatology. *J. Hydrol.* **189**, 74–96 (1997).
- Owe, M., de Jeu, R. & Holmes, T. Multisensor historical climatology of satellite-derived global land surface moisture. *J. Geophys. Res.* **113**, F01002 (2008).
- Trigo, I. F., Monteiro, I. T., Olesen, F. & Kabsch, E. An assessment of remotely sensed land surface temperature. *J. Geophys. Res.* **113**, D17108 (2008).
- Stewart, D. J., Taylor, C. M., Reeves, C. E. & McQuaid, J. B. Biogenic nitrogen oxide emissions from soils: Impact on NOx and ozone over west Africa during AMMA (African Monsoon Multidisciplinary Analysis) observational study. *Atmos. Chem. Phys.* **8**, 2285–2297 (2008).
- Taylor, C. M., Harris, P. P. & Parker, D. J. Impact of soil moisture on the development of a sahelian mesoscale convective system: A case study from the AMMA special observing period. *Q. J. R. Meteorol. Soc.* **136**, 456–470 (2010).
- Taylor, C. M., Parker, D. J. & Harris, P. P. An observational case study of mesoscale atmospheric circulations induced by soil moisture. *Geophys. Res. Lett.* **34**, L15801 (2007).
- Gantner, L. & Kalthoff, N. Sensitivity of a modelled life cycle of a mesoscale convective system to soil conditions over West Africa. *Q. J. R. Meteorol. Soc.* **136**, 471–482 (2010).
- Gaertner, M. A., Dominguez, M. & Garvert, M. A modelling case-study of soil moisture–atmosphere coupling. *Q. J. R. Meteorol. Soc.* **136**, 483–495 (2010).
- Chen, F. & Avissar, R. Impact of land-surface moisture variability on local shallow convective cumulus and precipitation in large-scale models. *J. Appl. Meteorol.* **33**, 1382–1401 (1994).
- Baidya Roy, S., Weaver, C. P., Nolan, D. S. & Avissar, R. A preferred scale for landscape forced mesoscale circulations? *J. Geophys. Res.* **108**, 8854 (2003).
- Weaver, C. P. Coupling between large-scale atmospheric processes and mesoscale land–atmosphere interactions in the US Southern Great Plains during summer. Part I: Case studies. *J. Hydromet.* **5**, 1223–1246 (2004).
- Pielke, R. A. *et al.* Nonlinear influence of mesoscale land-use on weather and climate. *J. Clim.* **4**, 1053–1069 (1991).
- Mathon, V. & Laurent, H. Life cycle of Sahelian mesoscale convective cloud systems. *Q. J. R. Meteorol. Soc.* **127**, 377–406 (2001).
- Carleton, A. M. *et al.* Summer season land cover—convective cloud associations for the Midwest US ‘Corn Belt’. *Geophys. Res. Lett.* **28**, 1679–1682 (2001).
- Wang, J. F. *et al.* Impact of deforestation in the Amazon basin on cloud climatology. *Proc. Natl Acad. Sci. USA.* **106**, 3670–3674 (2009).
- García-Carreras, L. *et al.* Impact of mesoscale vegetation heterogeneities on the dynamical and thermodynamic properties of the planetary boundary layer. *J. Geophys. Res.* **115** (2010).
- García-Carreras, L., Parker, D. J. & Marsham, J. H. What is the mechanism for the modification of convective cloud distributions by land surface–induced flows? *J. Atmos. Sci.* **68**, 619–634 (2011).
- Morel, C. & Senesi, S. A climatology of mesoscale convective systems over Europe using satellite infrared imagery. I: Methodology. *Q. J. R. Meteorol. Soc.* **128**, 1953–1971 (2002).
- Foster, G. Wavelets for period analysis of unevenly sampled time series. *Astronomical J.* **112**, 1709–1729 (1996).

Acknowledgements

Based on a French initiative, AMMA was built by an international scientific group and is currently funded by a large number of agencies, especially from France, the UK, the US

1 and Africa. The authors were funded by the European Community's Sixth Framework
2 Research Programme and the UK NERC project NE/B505597/1. We would like to thank
3 D. Parker and J. Polcher for many valuable discussions on this topic. We also thank
4 LandsAF for the provision of land surface temperature data, EUMETSAT for cloud data,
5 and R. de Jeu for soil moisture retrievals.

6 Author contributions

7 C.M.T. and F.G. conceived the study and wrote the paper, A.G. analysed the LST
data, C.M.T. developed the cloud tracking, F.G. determined the atmospheric

sensitivities, P.P.H. devised statistical tests, R.J.E. and F.C. evaluated the tracking
and M.D.K. performed the wavelet analysis. All authors discussed the results and
commented on the manuscript.

Additional information

The authors declare no competing financial interests. Supplementary information
accompanies this paper on www.nature.com/naturegeoscience. Reprints and permissions
information is available online at <http://www.nature.com/reprints>. Correspondence and
requests for materials should be addressed to C.M.T.

8
9
10
11
12
13
14
15

Page 1

Query 1: Line no. 1

Please note that the first paragraph has been edited according to style.

Query 2: Line no. 47

Please provide full postal address and postcode for all affiliations

Page 2

Query 3: Line no. 1

There could be some confusion in Figure 1. 'Each horizontal line represents one decile, a circle indicates the median' (ok there are 10 of them in each figure) ', and shading delimits the 95% confidence limits' (do you want to define the dashed line as well? To make sure no one thinks that is the earlier lines mentioned.)

Query 4: Line no. 51

Should the word 'analysis' be added after 'microwave'?

Page 3

Query 5: Line no. 44

Would 'the next two days' be better than 'the following day or two.'